Burst mode with ps- and fs-pulses: Influence on the removal rate, surface quality and heat accumulation

B. Neuenschwander*, Th. Kramer, B. Lauer, B. Jaeggi
Bern University of applied Sciences, Institute for Applied Laser, Photonics and Surface Technologies, Pestalozzistrasse 20, 3400 Burgdorf, Switzerland

ABSTRACT

The burst mode for ps and fs pulses for steel and copper is investigated. It is found that the reduction of the energy in a single pulse (in the burst) represents the main factor for the often reported gain in the removal rate using the burst mode e.g. for steel no investigated burst sequence lead to a higher removal rate compared to single pulses at higher repetition rate. But for copper a situation was found where the burst mode leads to a real increase of the removal rate in the range of 20%. Further the burst mode offers the possibility to generate slightly melted flat surfaces with good optical properties in the case of steel. Temperature simulations indicate that the surface state during the burst mode could be responsible for the melting effect or the formation of cavities in clusters which reduces the surface quality.

Keywords: burst mode, heat accumulation, surface quality, micromachining, ultra – short pulses

1. INTRODUCTION

Ultra – short laser pulses have shown their applicability for high quality laser micromachining of metals, semiconductors and insulators in manifold applications. However, to really enter into the large field of industrial applications the demand of high throughput still represents one of the key factors. It was shown, especially for metals, that the efficiency of the ablation process can be optimized i.e. that there exists a maximum removal rate per average power[1,2]. This maximum depends on the pulse duration[3,4,5,6] whereas shorter pulses lead to higher removal rates. As working at this maximum point usually demands moderate fluences (typically in the range of 1 J/cm^2 or less) multi – spot processing or high speed scanning represent potential technologies to work at high average powers.

Diffractive optical elements (DOE's) can be used to generate a pattern with a defined number of spots allowing parallel processing of identical structures in the dimension of the spot separation. Variable DOEs like spatial light modulators offer more flexibility for laser micro machining but are limited today in speed at about 50 Hz refresh rate and also in pulse energy and average power of approximately 50 W.

Fast scanning represents another approach to fulfill the demands of micromachining with high average power. High surface speeds are e.g. offered by fast rotating cylinders which can either be combined with additional acousto-optic deflectors[7] or be completely synchronized with the laser system[8,9]. A more flexible approach are polygon line scanners offering marking speeds of 100 m/s and higher as well as the possibility of a synchronization with the laser system[10]. Due to their high marking speed these systems offer the possibility to work at average powers exceeding 100 W. Results with a 50 W ps-laser-system are reported in[11]. In[12] it is shown that neither heat accumulation nor plasma – shielding significantly influences the removal rate and machining quality for different steel grades.

Moderate fluences in a single pulse at high average powers can also be obtained using pulse bursts. Most ultra – short pulsed high power systems are arranged in a MOPA set – up with a seed oscillator working in the MHz regime and one or a sequence of multi – path amplifiers which facilitates the generation of pulse bursts. In the burst mode the first pulse picker, reducing the repetition f_S rate of the seed oscillator to the desired repetition rate f_L of the laser system, is capable of letting pass not only single pulses but a sequence of n pulses as illustrated in fig. 1. The bursts are following each other

*beat.neuenschwander@bfh.ch; phone +41 34 426 42 20; laserlab.ti.bfh.ch

source: https://doi.org/10.24451/arbor.16031 | downloaded: 15.4.2020

still with the repetition rate of the laser with a time spacing of $\Delta t_L = 1/f_L$ whereas the time spacing between the pulses in the burst is given by the repetition rate of the seed oscillator $\Delta t_B = 1/f_S$. The highest possible number n of pulses in a burst and their time spacing Δt_B depend on the used laser system. Most systems offer the possibility to suppress single pulses in the burst sequence which can e.g. be used to vary the time spacing between the pulses in the burst in multiples of Δt_B. Furthermore the energy of the pulses in the burst typically continuously drops with the first pulse having the highest energy unless further actions are taken; e.g. the FlexBurst™ technology offers the possibility to individually adjust the energy of every single pulse in the burst.

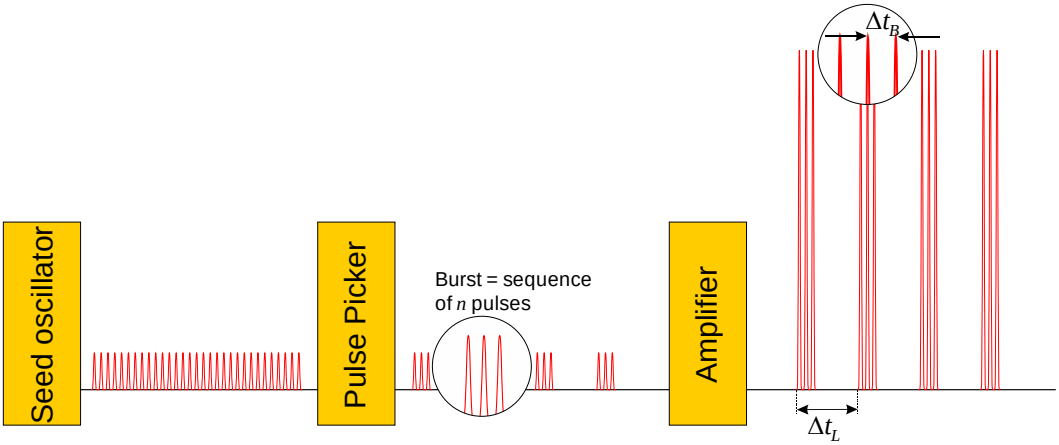

Figure 1. Scheme of burst generation. The first pulse picker lets pass series of n pulses from the seed oscillator.

Allthough bursts for ultra – short pulsed lasers are known for years, systematic studies for laser micromachining with bursts are only rarely published. In the case of glasses bursts are used e.g. for welding[13], writing of gratings or waveguides[14,15] or cutting based on filamentation[16]. For steel C75 and 12 ps pulses the influence of Δt_B was investigated for two pulse bursts[17]. It was shown, that for a two pulse burst the specific removal rate is slightly higher than for one pulse containing twice the energy of a pulse in the burst but the surface roughness strongly depends on Δt_B. Up to 14 times higher specific removal rates compared to single pulses were reported for an 8 or 10 pulse burst when machining tungsten carbide and silicon[18]. For stainless steel still a 10 times higher specific removal rate was observed as illustrated in fig. 2a). allthough simulations with the two-temperature-model for Cu predicts higher removal rates using bursts[19] this reported enormous increase is mainly caused by another effect. In the reported case where relatively low repetition rates at high average powers were used the fluence of a single pulse in the burst is much closer to the optimum fluence and pulse energy with maximum specific removal rate[1,2] compared to the very high fluence resulting for a pulse containing the same energy as the whole burst train. This fact is illustrated in fig. 2b) and compared with a model function (1) which will be introduced in section 2.

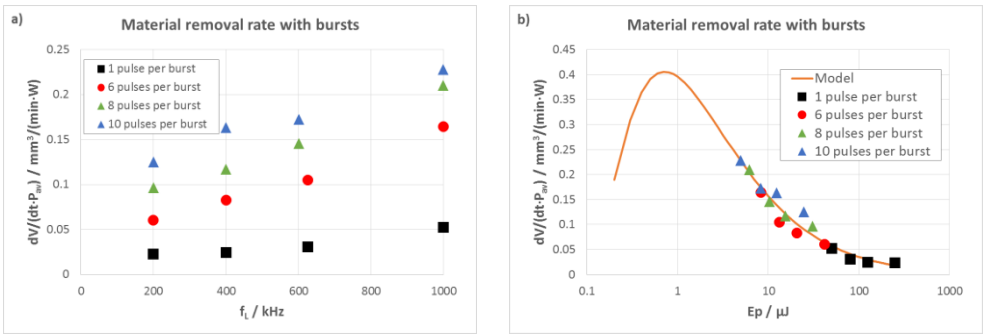

Figure 2: Obtained specific removal rates in stainless steel[18] with 50 W average power: a) as a function of the laser repetition rate and b) as a function of the pulse energy per single pulse in the burst.

In a systematic study it has therefore to be distinguished between the influence of the pulse energy of a single pulse in the burst and additional effects, as e.g. heat accumulation, which are caused by the short time spacing Δt_B of the pulse sequence in a burst.

2. THEORETICAL MODELS

2.1 Specific removal rate

Based on the often reported law[20,21] where the ablation depth logarithmically depends on the applied fluence the specific removal rate per average power can be calculated[11] as follows:

$$\frac{\dot{V}}{P_{av}} = \frac{1}{2} \cdot \frac{\delta}{\phi_0} \cdot \ln^2\left(\frac{\phi_0}{\phi_{th}}\right) \quad \text{with:} \quad \phi_0 = \frac{2 \cdot E_P}{\pi \cdot w_0^2} \tag{1}$$

Where δ denotes the energy penetration depth, ϕ_{th} the threshold fluence, ϕ_0 the peak fluence (in the center of the Gaussian beam), E_p the pulse energy and w_0 the spot radius. The model function in fig. 2b) represents the least square fit of (1) to the data with w_0 = 11 µm, ϕ_{th} = 0.051 J/cm^2 and δ = 12.8 nm.

2.2 Heat Accumulation

Even for ultra – short pulses a part of the deposited energy rests in the bulk material and heat accumulation may become an issue. Scanning a pulsed laser beam along a line can lead to heat accumulation if the pitch (distance between the pulses) is too small or if a very high repetition rate in the MHz regime is used. For steel 1.4301 (AISI 304) it was shown[22] that about 40% of the laser energy rests in the solid material and that the formation of bumpy surfaces occurs for scan speeds below a critical value depending on the average power and the repetition rate. As this critical value itself depends on the base temperature of the sample it is assumed that the formation of bumps is a temperature depending effect. The surface temperature just at the time when the next pulse strikes the surface is estimated by numerical simulations and an analytical model. It is shown that the critical speed for bump formation directly corresponds to a threshold temperature of about T_{th} = 610°C. An analytic expression for the temperature distribution of an instantaneous Gaussian shaped heating pulse allows estimating the surface temperature of a scanned pulsed laser beam also in burst mode. For a single pulse impinging on the surface at t = 0 at the location (x_0, y_0, 0) the temperature raise reads[22]:

$$T^{s.p.}_{(x_0,y_0)}(x,y,z,t) = \frac{2E_{res}}{\pi\rho c\sqrt{\pi\kappa t}(8\kappa t + w_0^2)} \cdot e^{\frac{(x-x_0)^2+(y-y_0)^2}{4\kappa t}\cdot\left(\frac{w_0^2}{8\kappa t + w_0^2} - 1\right)} \cdot e^{-\frac{z^2}{4\kappa t}} \tag{2}$$

With E_{res} the residual energy, ρ the density, c the specific heat and κ the thermal diffusivity. For a burst with n pulses scanned with velocity v along the x-axes the temperature distribution then reads:

$$T^{b}_{(x_0,0)}(x,y,z,t) = \sum_{i=0}^{n-1} T^{s.p.}_{(x_i,0)}(x,y,z,t_i) \tag{3}$$

With $x_i = x_0 - i \cdot \frac{v}{f_S}$, $t_i = t - i \cdot \Delta t_B$ if burst pulse i is already emitted and Δt_B the time spacing between the pulses in the burst. The temperature distribution of the last N burst sequences is then given by:

$$T_{(x_0,0)}(x,y,z,t) = \sum_{m=0}^{N} T^{b}_{(x_{0,m},0)}\left(x,y,z,t + \frac{m}{f_L}\right) \tag{4}$$

With $x_{0,m} = x_0 + m \cdot \frac{v}{f_L}$ and f_L the repetition rate of the laser. Expressions (2)-(4) allow to estimate the heat accumulation along a straight scan line for a burst mode.

3. EXPERIMENTAL SET – UP

On the one hand a FUEGO System from JDSU with more than 40 W average power at its fundamental wavelength of 1064 nm and a pulse duration of 10 ps was used for the experiments. It offers the possibility to adjust the energy of each individual pulse in a burst and bursts with up to 8 pulses can be selected. Based on the seed laser's repetition rate of 82 MHz the time spacing Δt_B between two pulses in a burst amounts about 12 ns. On the other hand a 5 W SATSUMA fs – laser from Amplitude – Systèmes with a fundamental wavelength of 1030 nm was used. Here the pulse duration amounts about 350 fs and the number of pulses in a burst is free. The time spacing between two pulses in a burst amounts to 20 ns and the energy per pulse in the burst sequence is decreasing.

With both systems squares with s = 1 mm, 1.6 mm or 2 mm side length were machined into metal targets. In the case of ps pulses a synchronized galvo scanner set – up[9] with identical pitch p in x- and y-direction was used. For the fs pulses a conventional hatching strategy with equal pitch and hatch distance was applied and the hatch angle was turned by 17°

from slice to slice. The spot radii were w_0 = 16 µm for the ps pulses and w_0 = 12 µm for the fs pulses. In both cases the laser repetition rate f_L, the pitch p, the number of slices N_{Sl} and the depth d of the squares, measured with a white light interference microscope (smart WLI from gbs), defines the removal rate per average power (= specific removal rate) or removed volume per pulse energy:

$$\frac{\dot{V}}{P_{av}} = \frac{\Delta V}{E_p} = \frac{d \cdot p^2}{N_{Sl}} \cdot \frac{f_L}{P_{av}} = \frac{d \cdot p^2}{N_{Sl}} \cdot \frac{1}{E_p} \tag{5}$$

A systematic study on 50 x 50 x 2 mm steel 1.4301 (AISI 304) and copper DHP (C12 200) plates was performed with the set – up for ps pulses. The copper plates were grinded and polished with 3 µm diamond paste whereas surface of the steel plates rested untreated. For a given repetition rate f_L, pitch p and number of pulses n of equal energy in a burst a sequence of squares with increasing pulse energy E_p was machined. It is noted here that the marking speed v is then given by $v = p \cdot f_L$. To guarantee a constant number of single pulses per unit area the number of slices N_{Sl} was adapted concerning the number of pulses per burst and the pitch. E.g. for a pitch of 8 µm and single pulses 192 slices were machined whereas only 8 slices are necessary for 6 pulses per burst and a pitch of 4 µm. The obtained specific removal rates per average power (5) should principally follow (1) and allow to compare different situations. The surfaces were partially monitored with an optical microscope and an SEM.

With the fs laser only steel 1.4301 was investigated. With 1, 2, …,8 and 10 pulses per burst and a pitch of 3, 6 and 9 µm squares were machined at 750, 500, 250, 167, 125, 100, 83 and 71 kHz repetition rate and with 90 slices. With a pulse energy of 1 µJ the fluence was near at its optimum value going with the highest specific removal rate for single pulses. The average power then was adjusted according to the repetition rate and number of pulses per burst. It has to be noted here that for the fs system the energy per pulse decreases in the burst sequence i.e. the first pulse in the burst contains the highest energy, the second pulse the second highest energy etc. As the pulse energy is only in average 1 µJ per pulse, the first pulse in the burst sequence has therefore an energy exceeding 1 µJ and this "overshoot" increases with the number of pulses per burst.

4. EXPERIMENTAL RESULTS

4.1 Steel, ps: Scale – up with single pulses

In a first experimental series single pulses at different repetition rates were investigated. Fig. 3a) shows the deduced specific removal rates for a pitch of 8 µm, 192 slices and a repetition rate of 200 kHz. It is obvious that for higher fluences the values are significantly lower than the ones predicted by the model. This does not change when the repetition rate and the corresponding average power are raised to 8 times higher values as illustrated in Fig. 3b). For all investigated repetition rates the same behavior is observed i.e. the ablation process is scalable in this regime and the results from the burst studies can directly by compared with results for single pulses at 200 kHz.

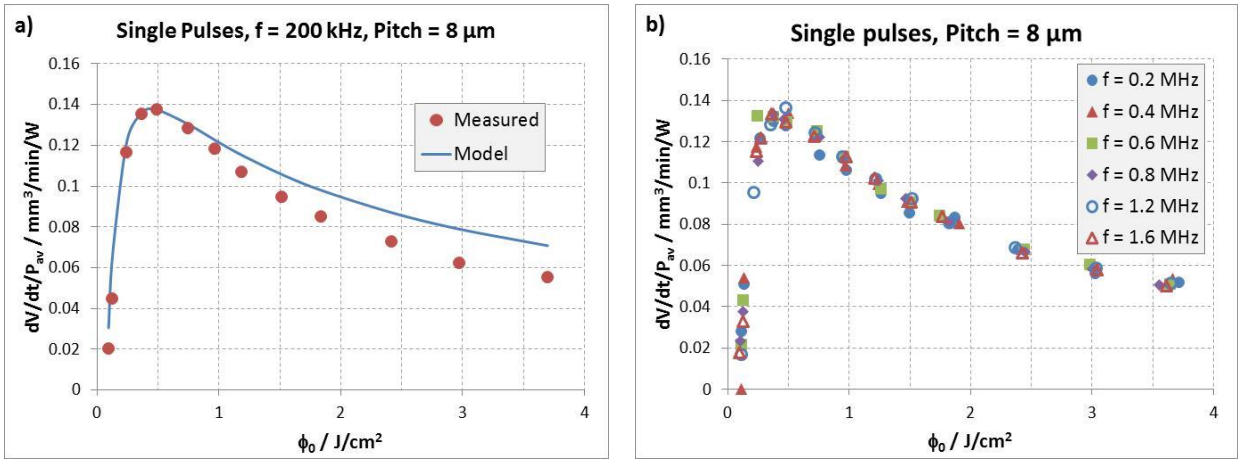

Figure 3. Specific removal rates per average power for single pulses. a) Measured values (red dots) and model function following (1). b) Measured values for different repetition rates from 200 kHz up to 1.6 MHz with constant pitch.

Microscopic images of the surfaces corresponding to Fig. 3a) are shown in Fig. 4, on the left for the optical microscope and on the right for the SEM. On the left side the applied peak fluence (1) is given in units of the optimum peak fluence. It can be seen, that around the optimum peak fluence a good machining quality respectively surface quality is obtained. When the fluence is raised to about 2 times the optimum value of about 0.4 J/cm^2, the formation of small cavities starts. These cavities are arranged in clusters which increase in area and cavity size when the fluence is further raised. When the peak fluence reaches about 7 times the optimum value the whole surface is covered by cavities. The peak fluence regime where the formation of cavities starts coincides with the peak fluence where the deviation from the deduced specific removal rates and the model starts, hence the drop below the predicted values is assumed to be caused by this cavity formation which negatively influences the ablation process and also strongly reduces the surface quality. Also for the higher repetition rates, the surface qualities show exactly the same trend and no significant difference between the repetition rates can be observed. A simulation of the surface temperature just before a pulse will strike on the surface leads to a maximum temperature raise (2,3,4) of about 62 °C for 200 kHz and 155 °C for 1.6 MHz which is far below the critical temperature of 610 °C[22]. Therefore one can finally conclude that working with peak fluences higher than twice the optimum value will lead to bad surface qualities and the ablation efficiency will decrease as well.

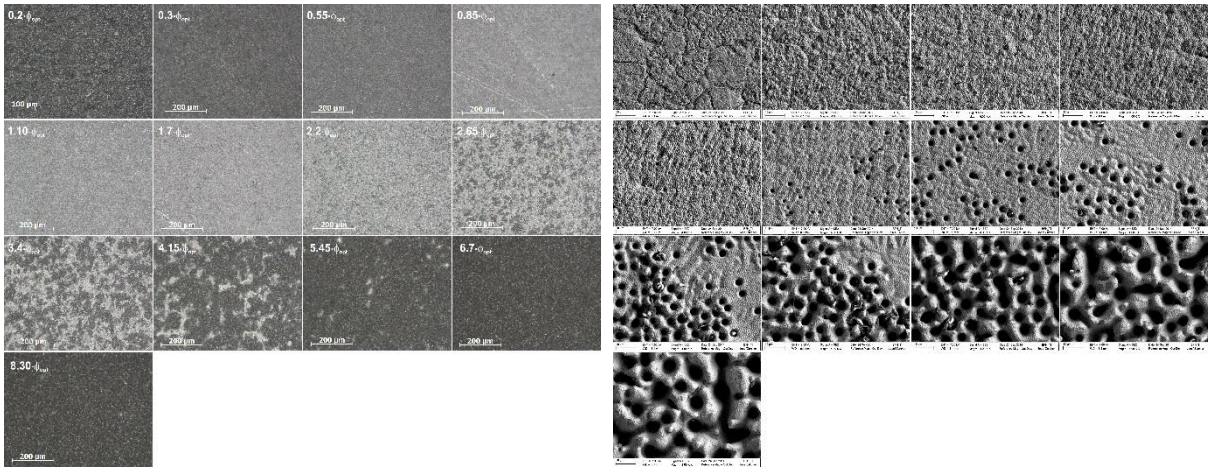

Figure 4. Microscopic images of the surfaces machined with single pulses, 192 slices at f = 200 kHz and a pitch of 8 µm. Each image corresponds to a measurement value of fig. 3a). Left: Optical microscope with the corresponding peak fluence in units of the optimum value. Every image shows a detail of 710 x 530 µm. Right: SEM-images showing details (290 x 200 µm) of the surfaces.

4.2 Steel, ps: Influence of the number of pulses per burst and the time spacing

In[18] an enormous increase in the removal rate using bursts with different numbers of pulses was reported by just taking the repetition rate into account. But for a fair comparison an 8 pulse burst at 200 kHz should be compared with single pulse at 1.6 MHz or a 3 pulse burst (at 200 kHz) with a single pulses at 600 kHz. In this case the pulse energy of every single pulse and the average power is identical and this allows a direct identification of the real influences of the burst mode. But as shown in Fig. 3b) there is no influence of the repetition rate on the specific removal rate for single pulses within the limits of experimental accuracy. Therefore all comparisons shown in the following figures were made at 200 kHz for single pulses The influence of the time spacing Δt_B between two pulses was investigated for 2, 3 and 4 pulses per burst at 200 kHz, a pitch of 8 µm and 96, 64 and 48 slices, respectively. The specific removal rates are compared with the results for single pulses and 192 slices. Fig. 5 shows the results for the 2 pulse and 3 pulse burst. In both cases the shortest time spacing of Δt_B = 12 ns leads to a drop in the maximum specific removal rate of about 20% for the 2 pulse burst and 25% for the 3 pulse burst. This drop is significantly reduced for the longer time spacing Δt_B = 24 ns and even vanishes for the 2 pulse burst for Δt_B = 36 ns whereas a small difference still rests for the 3 pulse burst in this situation. Further the reduction in the specific removal rate shifts the optimum fluence to higher values. Similar behavior was also observed for a 4 pulse burst where 12 ns and 24 ns time spacing was investigated. A first assumption is that the observed reduction is caused by plasma shielding i.e. the consecutive pulse in the burst is partially shielded by the plasma produced by the previous pulse. But other experiments[34] have shown that plasma shielding should

be strongest about 40 – 50ns after the pulse and therefore further investigations are needed to clarify the reason for this reduction.

In fig. 6 the deduced specific removal rates for different numbers of pulses in a burst with a time spacing of Δt_B = 12 ns are presented. No combination of bursts lead to a higher specific removal rate than single pulses at the optimum point i.e. the highest removal rate is always obtained with single pulses. But if one is not able to work at the optimum point with moderate fluences and applies much higher energies, then a pulse burst can lead to a higher removal rate e.g. in fig. 5a at a peak fluence of about 3.5 J/cm^2 the specific removal rate of an 8 pulse burst is about twice as high as for single pulses.

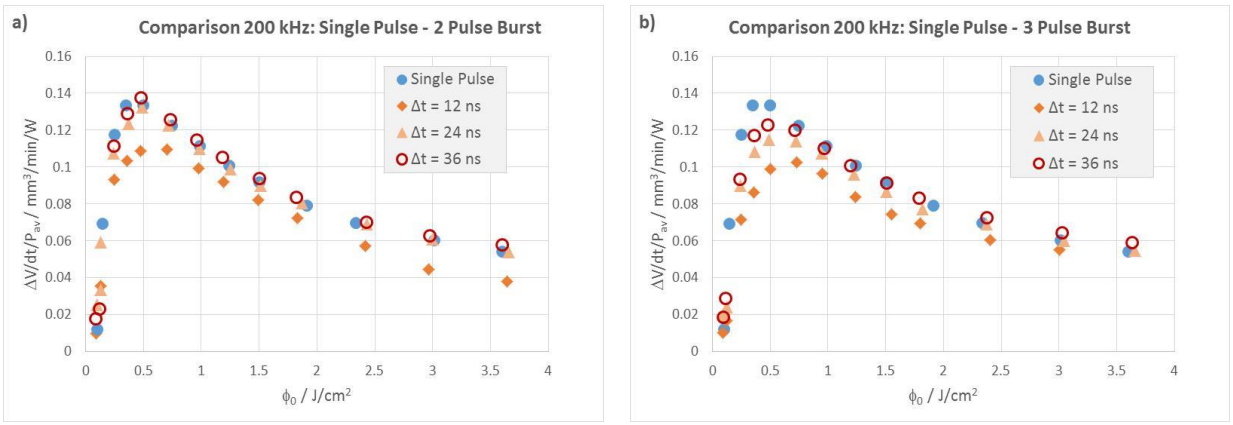

Figure 5. Specific removal rates for different time spacing between the burst pulses for a 2 pulse burst a) and a 3 pulse burst b).

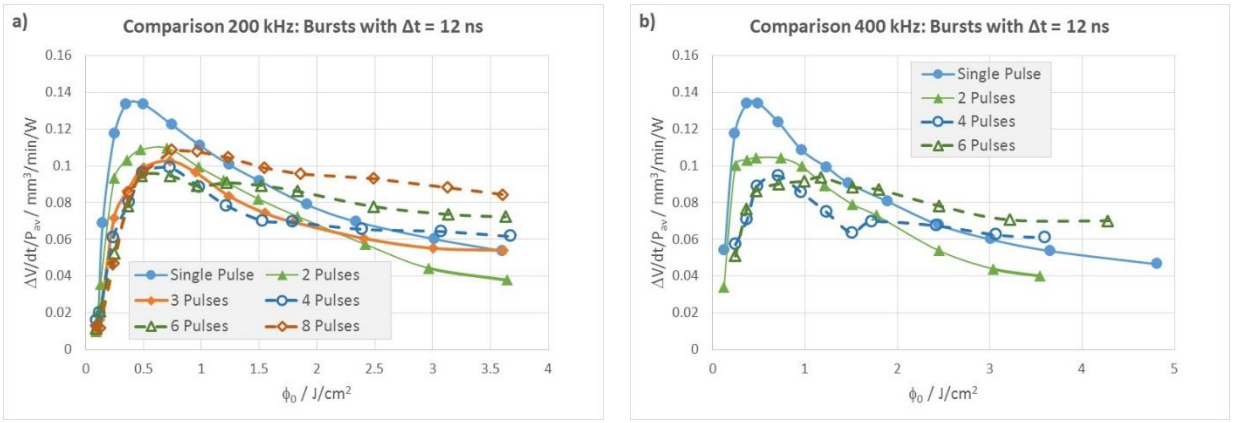

Figure 6. Specific removal rates for different number of pulses in a burst at a repetition rate of 200 kHz a) and 400 kHz b). The solid lines represent guides to the eye.

The number of pulses in a burst has a strong influence onto the surface quality as illustrated in fig. 7. For special combinations a small surface melting effect, leading to a flat shiny surface, occurs. For the 3 pulse burst with a time spacing of 12 ns a quite wide process window for shiny surfaces between ϕ_{opt} and about $2.5 \cdot \phi_{opt}$ exists. For higher number of pulses this process window becomes narrower and is shifted towards lower fluences. Within this process window a thermal coloring can be observed for the higher fluences. For the 2, 3 and 4 pulse bursts a further rise of the fluence will lead to formation of cavities arranged in clusters. In the case of the 4 pulse burst the cavities disappear for higher fluences and for the 6 and 8 (not shown here) pulse burst no formation of cavities is observed. But in both cases the surface becomes black and rough.

In addition the influence of the pitch was investigated. In general the reduction of the pitch leads to stronger blackening and rough surfaces. Even parameters do exist where a shiny surface can be realized with a small melting effect, the corresponding process windows were quite narrow. For single pulses the reduction of the pitch from 8 µm to 1 µm lead to an increase of the removal rate in the range of 10 – 20% but this does not compensate the lower surface quality.

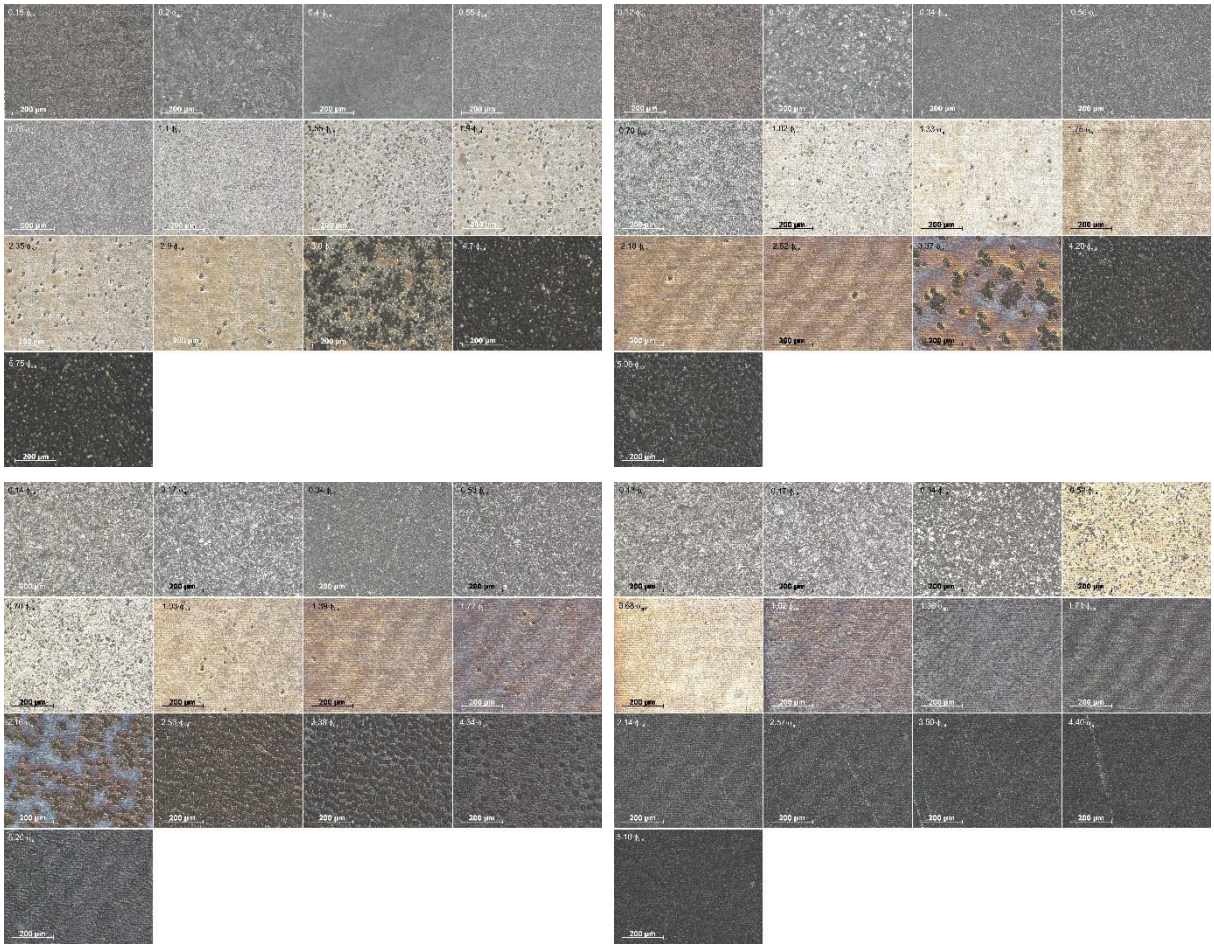

Figure 7. Microscopic images showing details (710 x 530 µm) of the machined surfaces at a repetition rate of 200 kHz and a pitch of 8 µm as a function of the peak fluence, given in units of the corresponding optimum peak fluence, for a 2 pulse burst (upper left), 3 pulse burst (upper right), 4 pulse burst (lower left) and 6 pulse burst (lower right) with a time spacing of 12 ns.

4.3 Copper, ps: Influence of the number of pulses per burst and the time spacing

An almost completely different situation is observed for copper. Figure 8 shows the results for single pulses, a pitch of 8 µm and a repetition rate of 200 kHz. In contrast to steel the measured values are in a very good agreement with the model function (1), the least square fit leads to $\phi_{th} = 0.36$ J/cm^2 and $\delta = 29.7$ nm. It has to be noted here, that for the lowest three fluences the random shift of the starting point[9] was set to zero leading to a periodic structure on the bottom of the squares. Additionally the development of a wavy surface with long period in the horizontal (scan) direction and short period in the vertical (cross scan) direction occurs when the fluence is raised. The periods seem not to depend on the applied fluence but the amplitude increases with the fluence. For fluences exceeding about twice the optimum (with maximum removal rate) a strong oxidation is observed and for the highest fluence at the border of the structure the formation of cavities starts. At the optimum fluence the surface quality is still good without oxidation and only small amplitudes in the wavy surface.

The investigation of the burst mode with different numbers of pulses in a burst and fixed time spacing of $\Delta t_B = 12$ ns show surprising results as illustrated in fig. 9:

For a two pulse burst the specific removal rates drops down to about 40% of the maximum value for single pulses. For an increasing peak fluence, the specific removal rate first increases, reaches a plateau where it almost rests at a value of about 40% of the single pulse maximum and finally slightly drops for the highest peak fluences. The surface at the

fluence with the highest specific removal rate is already oxidized and becomes brown (see right part of fig. 9). A reduction of the specific removal rate has also been observed for steel, but it was with about 20% much lower tan the 60% obtained for copper.

The really surprising result is then observed for the 3 pulse burst. For steel a reduced specific removal rate was obtained, but for copper the maximum specific removal rate exceeds the maximum values from single pulses by about 20% which is significant. At this peak fluence also the surface quality is quite good, it seems to be only little oxidized. For higher fluences the specific removal rates become smaller than the values obtained for single pulses.

For the 4 pulse burst the specific removal rate rests always below the maximum obtained for single pulses and for 6 pulses per burst the maxim specific removal rate equals the one for single pulses, but is reached at twice the peak fluence (per pulse in the burst) compared to single pulses. For both situations the surface is rough and black due to oxidation leading to a bad quality.

For the 8 pulse burst finally the maximum removal rate is in the same range as for the 3 pulse burst but having a look at the surface it manifests its bad quality due to oxidation and roughness.

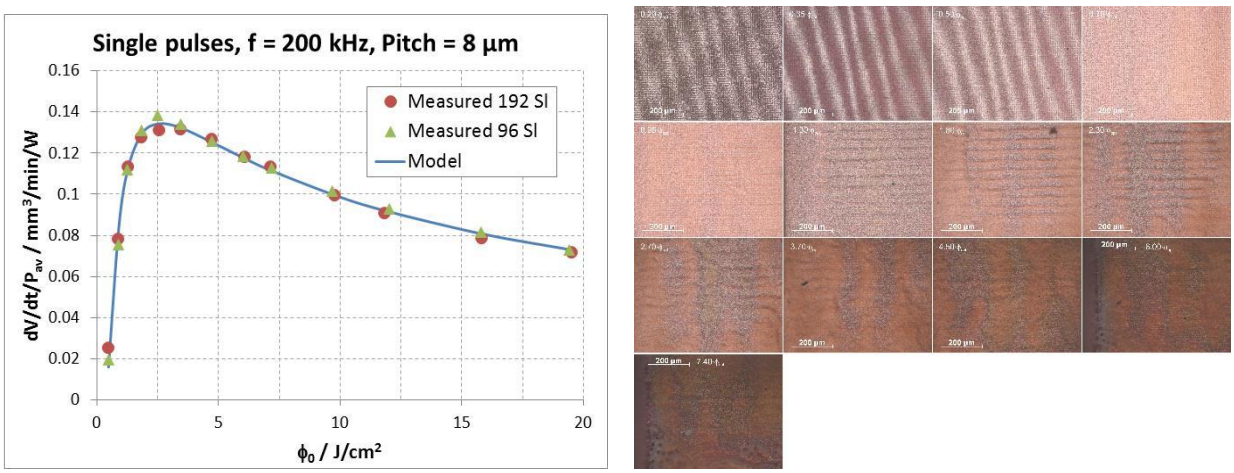

Figure 8: Specific removal rates measured for copper and single pulses (left) with 192 slices (red dots) and 96 slices (green triangles). The blue line represents the least square fit of the model to the data. Microscopic – images (right) showing details (710 x 530 µm) of the machined surfaces with 192 slices. The applied fluence is given in units of the optimum fluence.

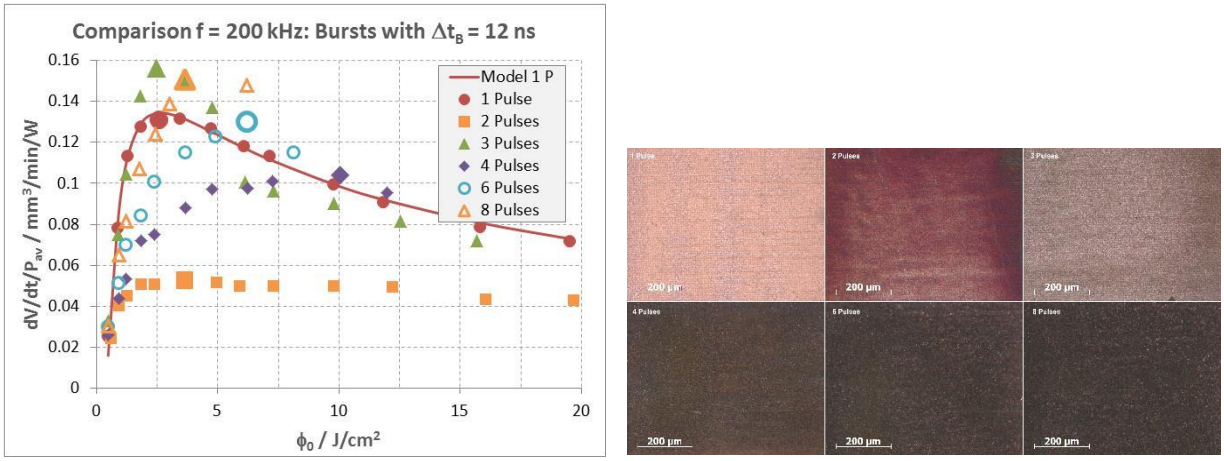

Figure 9: Specific removal rates measured for different numbers of pulses in a burst (left) with a constant time spacing of 12 ns. The increased markers denote the fluences with the highest specific removal rate. Right: Microscopic images showing details (710 x 530 µm) of the surfaces machine at the fluences with highest specific removal rate.

For 2, 3 and 4 pulses in the burst also the influence of the time spacing Δt_B was investigated. For a 2 pulse burst (fig. 2a)) the maximum specific removal rate slightly increases with the time spacing from 0.052 mm^3/min/W to 0.056 mm^3/min/W, 0.063 mm^3/min/W and 0.080 mm^3/min/W for 12 ns, 24 ns, 36 ns and 60 ns, respectively, but still rests far below the 0.13 mm^3/min/W obtained for single pulses. The contrary behavior is observed for a 3 pulse burst (fig. 10b) an a 4 pulse-burst (not shown here). When the time spacing is raised from 12 ns to 24 ns and 36 ns the maximum specific removal rate drops from 0.156 mm^3/min/W down to 0.126 mm^3/min/W and 0.112 mm^3/min/W. The latter two values are below the one for single pulses i.e. it would be more efficient to work with single pulses at the tripled repetition rate than with a 3 pulse burst with a time spacing of 24 ns or more.

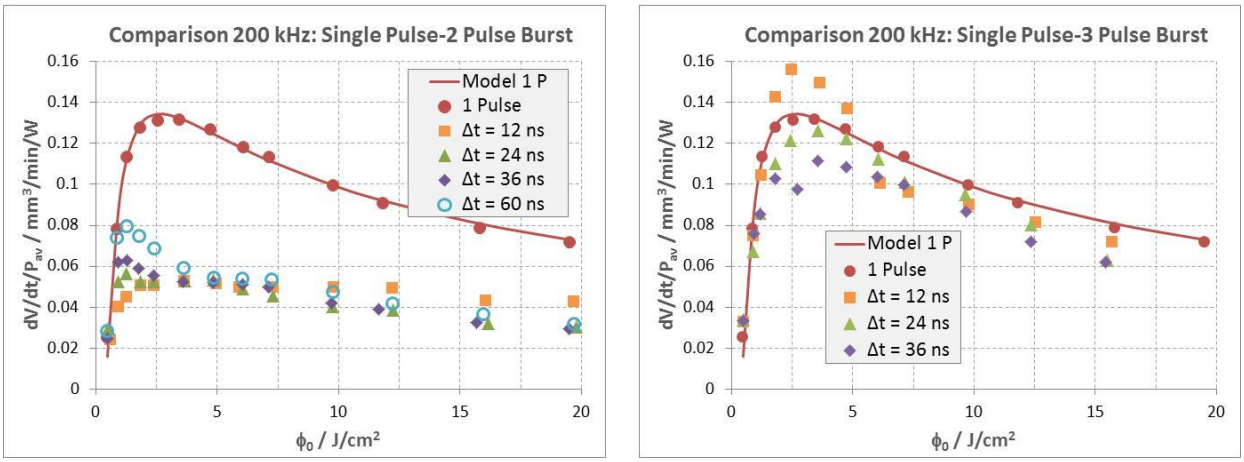

Figure 10: Specific removal rates as a function of the time spacing Δt_B between the burst pulses for a 2 pulse burst a) and a 3 pulse burst b) at a repetition rate of 200 kHz and a pitch of 8 µm.

Finally one can conclude that the specific removal rate for copper ideally follows the predicted model (1) for single pulses. In contrast to steel it is possible to increase the specific removal rate by about 20% using a 3 pulse burst with a time spacing of 12 ns.

4.4 Steel, fs: Influence of the burst mode

The results for fs pulses equals the one for ps pulses i.e. almost no significant difference was found for different repetition rates when the mean pulse energy, the pitch and the number of bursts was constant. Fig 11 shows the surfaces for selected situations. Increasing the number of pulses per bursts leads to a bumpy surface (see fig. 11 b) and c)) and finally to molten bumps resulting in a flatter surface. A too high fluence again leads to the formations of clusters of cavities (see fig. 11 d)). Due to the longer time spacing of 20 ns between the burst pulses and the limited pulse energy the melting effect (fig. 11 d)) was only observed for a few situations.

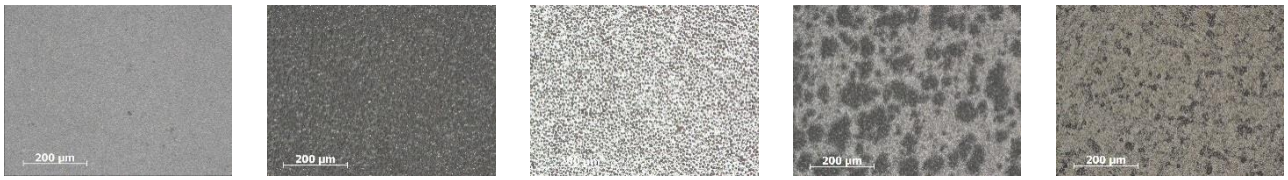

a) 1 pulse, 500 kHz, 0.5 W, p = 6 µm
b) 5 pulses, 500 kHz, 2.5 W, p = 6 µm
c) 10 pulses, 500 kHz, 5.0 W, p = 6 µm
d) 1 pulse, 500 kHz, 4.0 W, p = 6 µm
e) 6 pulses, 750 kHz, 3.1 W, p = 9 µm

Figure 11: Microscopic images showing details (710 x 530 µm) of different machined surfaces with fs laser pulses. a) - c): Mean pulse energy 1 µJ per pulse. d): Mean pulse energy 8 µJ per pulse. e): Mean pulse energy 0.69 µJ

5. SIMULATION RESULTS

The simulations were performed according to the presented model (2), (3) and (4). To avoid errors due to the instantaneous insertion of the energy and the energy transfer from the electrons to the lattice which is described by the two temperature model, the first 500 ps after impinging of the pulse, also in a burst sequence, are not calculated. As the simulations do not take into account any phase transitions the calculated temperatures are afterwards transformed according to the specific heat of melt and evaporation. Temperature dependencies of the material parameters as well as heat losses due to radiation and convection are not taken into account. It is therefore assumed that the calculated temperatures could be too high, either.

First the temperature on the x-axis just before the next burst sequence impinges at position x = 0 was investigated. For repetition rates in the range of a few 100 kHz there was no significant difference observed between a burst with n pulses and a single pulse with containing n times the energy of a pulse in the burst, i.e. for heat accumulation effects the burst pulse can be treated as a single pulse of n times higher energy. The situations changes when the burst is compared to a single pulse with the energy of a pulse in the burst but n times higher repetition rate. This fact is illustrated in fig. 12 where the temperatures for a 4 pulse burst, a single pulse containing a 4 times higher energy, a single pulse of equal energy but 4 times higher repetition rate and a single pulse of equal energy and repetition rate are calculated.

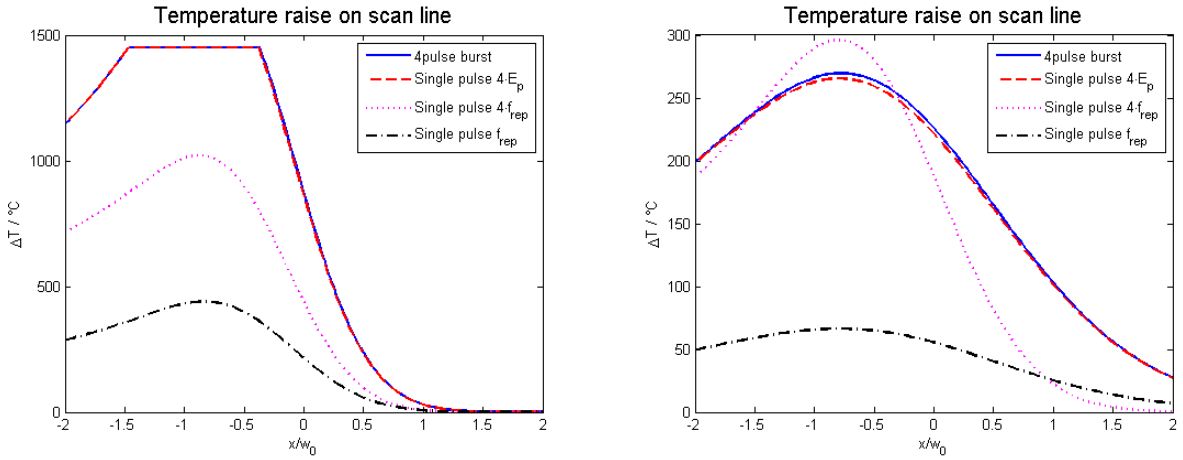

Figure 12: Temperature raise on the scan line for a 4 Pulse burst and a pitch of 8 µm just before the next burst sequence impinges on the surface. Left: For steel 1.4301 with 12 W average power and 500 kHz repetition rate. The "plateau" denotes the region where the melting temperature was achieved i.e. the material in this range is in the solid and in the liquid phase. Right: For Copper with 40 W average power and 1 MHz repetition rate. The distance x is given in units of the spot radius w_0 and as the previous pulse has struck the surface at x = -0.5 w_0 the maximum temperatures appear in this region.

The appearance of melting effects in steel is therefore assumed to be a consequence of the temperature dynamics during or shortly after the pulse burst. Corresponding calculations have been done and results are summarized for a 2 and a 3 pulse burst in fig. 13. It shows the evolution of the temperature distribution along the scan line but only for the first 5% of the time interval between two bursts i.e. the first 250 ns for the repetition rate of 200 kHz.

For a grey and slightly matt surface corresponding to the first images in both rows, the pulses in the burst seem to strike on a solid or not completely melted surface. Looking at the melted surface (image 2 in the first row and image 2 and 3 in the second row) suggests that at least one pulse has to strike on a completely molten surface. Finally the formation of cavities (images 3 and 4 in the first row and image 4 in the second row) appear when parts of the surface are completely vaporized. Further it can be shown that for the situation where the formation of cavities does not appear or disappears, the phase where parts of the surface are totally melted has a duration of more than half of the interval between two burst sequences i.e. 125 ns in the presented case. Taking into account that the calculated temperatures could be too high the following assumption is made: As long as the pulses in the burst strikes on a solid surface the surface rests grey and slightly matt. Due to heat accumulation it can oxidize and becomes black. If at least one pulse strikes on completely molten surface parts this leads to observed melting effect and if parts of the surface are fully vaporized the formation of cavities starts.

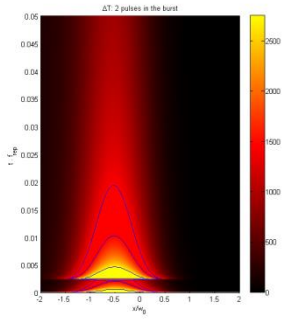

2 pulses, 1.1 W, img. 6 in fig 7
slightly matt surface

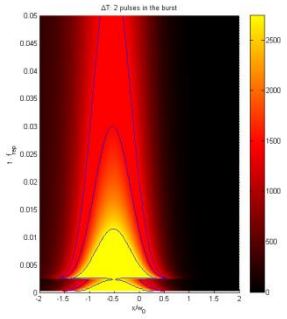

2 pulses, 1.9 W, img. 7 in fig. 7
melting starts

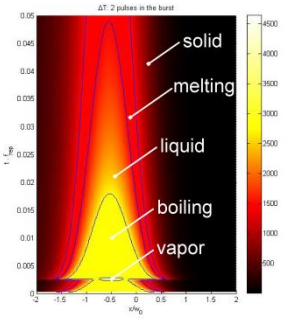

2 pulses, 2.4 W, img. 9 in fig. 7
molten, cavities

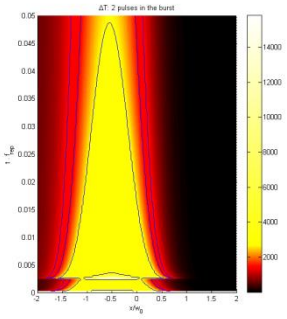

2 pulses, 3.9 W, img. 11 in fig. 7
molten and clusters with cavities

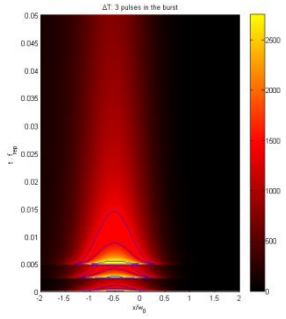

3 pulses, 0.9 W, img. 5 in fig. 7
slightly matt surface

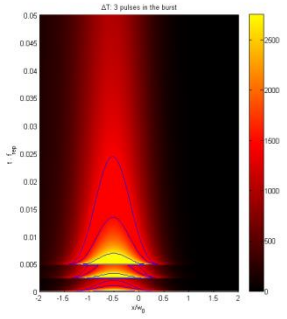

3 pulses, 1.2 W, img. 6 in fig. 7
melting just starts

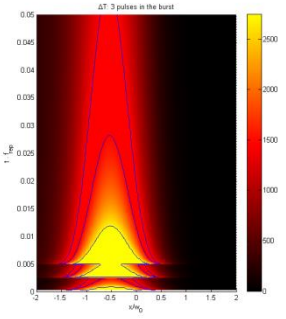

3 pulses, 1.8 W, img. 7 in fig. 7
molten

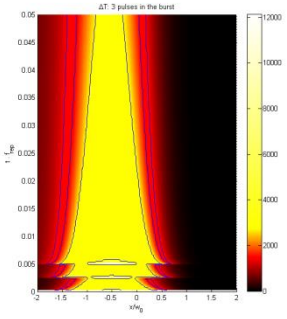

3 pulses, 4.4W, img. 11 in fig. 7
molten and clusters with cavities

Figure 13: Temporal evolution of the temperature distribution along the scan line for a 2 pulse burst (top) and a 3 pulse burst (bottom) and different average powers corresponding to specific situations shown in fig. 7. The position in units of the spot radius is shown on the x-axis where x = 0 denotes the position where the next pulse burst will strike the surface. The time in units of the time interval between two pulse bursts is shown on the y-axis. The solid lines denote the transition between the solid, melting, liquid, boiling and vapor phase.

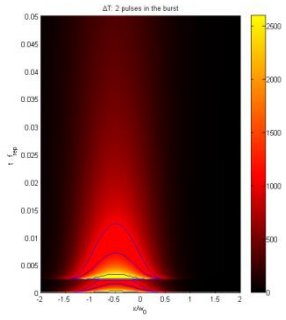

2 pulses, 3.9 W, 5th fluence fig. 9
Δt_B=12ns, no melting, oxidation

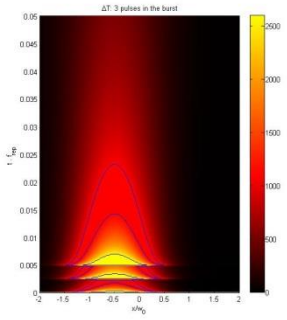

3 pulses, 6.0 W, 5th fluence fig. 9
Δt_B=12ns, no melting, highest rate

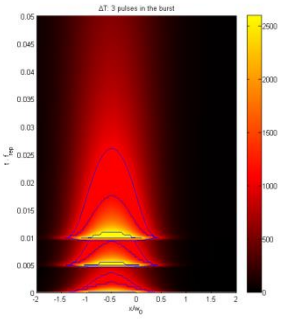

3 pulses, 6.0 W, 5th fluence fig. 9
Δt_B=24ns, no melting, highest rate

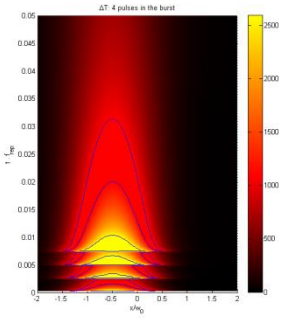

3 pulses, 6.0 W, 5th fluence fig. 9
Δt_B=12ns, no melting

Figure 14: Temporal evolution of the temperature distribution along the scan line for copper and different situations. The position in units of the spot radius is shown on the x-axis where x = 0 denotes the position where the next pulse burst will strike the surface. The time in units of the time interval between two pulse bursts is shown on the y-axis. The solid lines denote the transition between the solid, melting, liquid, boiling and vapor phase.

Results of simulations for copper are shown in fig. 14. The first image shows the temperature evolution of a two pulse burst. As it can be seen, the second pulse strikes only on a partially molten or even solid surface. For the three pulse burst the third pulse sees a completely molten surface. In[24] it is reported that for a wavelength of 10.6 µm the absorption of copper jumps discontinuously from 2% to 6% at the phase transition from solid to molten. If a similar jump will also be

present for wavelengths in the near IR this could explain the significantly higher removal rate obtained for a 3 pulse burst with 12 ns separation of the burst pulses. If the pulses are separated by 24 ns (third image in fig. 14) all pulses will strike on a solid or only partially molten surface. Taking further into account that the second pulse has a significant weaker absorption in the material due to much lower specific removal rate it is assumed that the surface will be in the solid phase for the third pulse in the burst with 24 ns spacing. The simulation for the 4 pulse burst now shows that in this situation the 3rd and the 4th pulse will see a completely molten surface and should therefore be quite efficient, which is definitively not the case. This could be explained with the quite bad energy coupling efficiency of the second pulse which should also appear for the 4th pulse taking into account that a 3 pulse burst is very efficient.

Fig. 15 a) shows the temperatures on the scan line for the burst sequences with 1, 3, 5, 7 and 10 fs pulses with a mean energy of 1 µJ at a repetition rate of 500 kHz. The critical temperature[22] for the generation of a bumpy surface is reached for 5 pulses in the burst. Here the surface is fully covered with bumps but its formation seems to start already at 3 pulses per burst where the maximum temperature is even below 400 °C. However, for 3 and 4 pulses per burst the bumps are clearly smaller than for 5 pulses per burst and their size even increases for higher number of pulses. Fig. 15 b) shows the temperature evolution during the 10 pulse burst. In a first approximation it can be assumed that for a n pulse burst the temperature evolution would look similar up to the nth pulse in the sequence. Taking into account the results for ps pulses the melting effect should start for 5 or 6 pulses per burst which is confirmed by the experiments as in fig. 11 b) first small molten parts can be identified. This melting becomes much more pronounced for a higher number of pulses per burst as can be seen in fig. 11c). The surface rests bumpy but no cavities are formed which could be explained by the missing vapor phase in fig. 15 b). Additionally the surface temperature for single pulses with an energy of 8 µJ at a repetition rate of 500 kHz is shown in fig. 15a). The maximum temperature amounts about to 900 °C and the corresponding surface (see fig. 11 c)) shows clusters of cavities as observed also for ps pulses. A slightly molten surface without cavities and bumps was obtained with a 6 pulse burst, a repetition rate of 750 kHz with an average power of 3.1 W and a pitch of 9 µm. The surface temperature just when the next burst strikes the surface shown in fig. 15 a) rests below the critical temperature whereas its evolution (see fig 15 c)) shows that the last three pulses of the burst sequence strikes on a completely molten or even boiling surface. Increasing now the energy per pulse or the number of pulses per burst would support the melting effect but at the same time the surface temperature would also exceed the critical value and the formation of cavities could start. The longer time spacing of 20 ns between the pulses in the burst may be responsible for the difficulties to find parameters for a slightly molten surface without formation of bumps or cavities in the case of fs pulses.

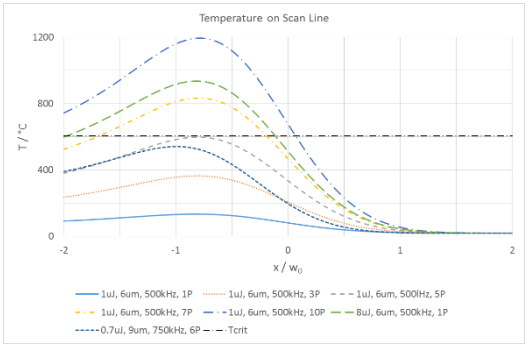

a)

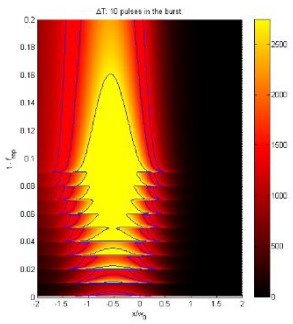

b) f = 500kHz, 10 pulses, p = 6 µm
P_{av} = 5 W

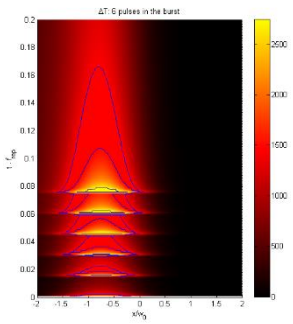

c) f =7 50kHz, 6 pulses, p = 9 µm
P_{av} = 3.1 W

Figure 15 a): Temperature on the scan line for different situations with fs pulses. b): Evolution of the temperature distribution on the scan line during 400 ns for a 10 pulse burst at 500 kHz. c): Evolution of the temperature distribution on the scan line during 270 ns for a 6 pulse burst at 750 kHz.

To back up all these assumptions more precise simulations e.g. FEM are necessary additionally taking into account heat losses due to radiation and convection as well as temperature dependent material parameters. Furthermore in the case of copper the energy coupling efficiency for the different pulses in the burst should also be considered.

6. CONCLUSION

The influence of the burst mode with ps and fs pulses on copper and steal was investigated. It was found that the enormous increase in the specific removal rate with bursts is mainly caused by the smaller energy in a single pulse of the burst which is nearer the optimum value for a maximum specific removal rate. However, the burst mode itself has an influence on the specific removal rate and the surface quality.

For steel the burst mode did never lead to a higher specific removal rate than single pulses with the optimum fluence. If one is forced to work at fluences exceeding the optimum value one will never get the maximum possible removal rate. It is in this situation where the burst mode may lead to higher (but always below maximum) efficiencies due to the possibility to generate slightly molten surfaces with high optical quality where single pulses would lead to cavity formation destroying the surface quality. Furthermore it is assumed that the state of the surface during the burst (solid, melting, liquid, boiling and vapor) strongly influences the surface quality.

For copper the specific removal rate strongly decreases for a 2 pulse burst whereas it exceeds the one for single pulses in the case of a 3 pulse burst. A real gain in the specific removal rate of about 20% seems to be possible in this case. This behavior could be explained by the almost doubled absorption of a liquid copper surface compared to the solid one. Nevertheless a significantly lower removal rate for a 2 pulse burst points to a shielding effect which reduces the energy coupling of the second and eventually also of the 4^{th} pulse.

Further investigations with 5 and 7 pulse bursts in the case of copper, eventually variable time spacing between the bursts, optimized energies in the single burst pulses and with more sophisticated simulations are necessary to get a better understanding of all the effects appearing when working in burst mode.

ACKNOWLEDGEMENTS

This work was supported by the European Union in the FP7 project APPOLO. Special thanks to Josef Zuercher for the help with the SEM Images.

REFERENCES

[1] Raciukaitis, G., Brikas, M., Gecys, P., Voisiat, B., Gedvilas, M., ”Use of high repetition rate and high power lasers in microfabrication: How to keep the efficiency high?,” JLMN journal of Laser Micro/Nanoengineering, 4, 186 (2009)

[2] Neuenschwander, B., Bucher, G., Nussbaum Ch.,, Joss, B., Muralt, M., Hunziker, U., Schuetz, P., ”Processing of metals and dielectric materials with ps-laserpulses: results, strategies, limitations and needs,” Proc. of SPIE, 7584, (2010)

[3] Schmid, M., Neuenschwander, B., Romano, V., Jaeggi, B., Hunziker, U., “Processing of metals with ps-laser pulses in the range between 10ps and 100ps,“ Proc. of SPIE, 7920, (2011)

[4] Jaeggi, B., Neuenschwander, B., Schmid, M., Muralt, M., Zuercher, J., Hunziker, U., “Influence of the pulse duration in the ps-regime on the ablation efficiency of metals,” Physics Procedia, 12B, 164-171 (2011)

[5] Lauer, B., Neuenschwander, B., Jaeggi, B.,Schmid, M., ”From fs – ns: influence of the pulse duration onto the material removal rate and machining quality for metals,” Proc. of ICALEO, M309, (2013)

[6] Lopez, J., Lidolff, A., Delaigue, M., Hönninger, C., Ricaud, S., Mottay, E., “Ultrafast Laser with high Energy and high average power for Industrial Micromachining: Comparision ps-fs,” Proc. of ICALEO, M401, (2011)

[7] Bruening, S., Hennig, G., Eifel, S., Gillner, A., ”Ultrafast Scan Techniques for 3D-Structuring of Metal Surfaces with high repetitive ps-laser pulses,” Physics Procedia, 12, 105-115 (2011)

[8] Jaeggi, B., Neuenschwander, B., Meier, B., Zimmermann, B., Hennig, G., ”High throughput laser micro machining on a rotating cylinder with ultra short pulses at highest precision,” Proc. of SPIE, 8607, (2013)

[9] Jaeggi, B., Neuenschwander, B., Meier, T., Zimmermann, M., Hennig, G., ”High Precision Surface Structuring with Ultra-Short Pulses and Synchronized Mechanical Axes,” Physics Procedia, 41, 319-326 (2013)

[10] De Loor, R., “Polygon scanner system for ultra short pulsed laser micro-machining applications,” Physics Procedia, 41, 544-551 (2013)
[11] Neuenschwander, B., Jaeggi, B., Zimmermann, M., Penning, L., De Loor, R., Weingarten, K., Oehler, A., ”High-throughput and high-precision laser micromachining with ps-pulses in synchronized mode with a fast polygon line scanner,” Proc. of SPIE, 8967, (2013)
[12] Neuenschwander, B., Jaeggi, B., Zimmermann, M., Hennig, G., ”Influence of Particle Shielding and Heat Accumulation Effects onto the Removal Rate for Laser Micromachining with Ultra-Short Pulses at High Repetition Rates,” Proc. of ICALEO, M1104, (2014)
[13] Zimmermann, F., Richter, S., Döring, S., Tünnermann, A., Nolte, S., “Ultrastable bonding of glass with femtosecond laser bursts,“ Appl. Opt., 52,1149 – 1154 (2013)
[14] Zhang, H., Eaton, S. M., Herman, P. R., “Single-step writing of Bragg grating waveguides in fused silica with an externally modulated femtosecond fiber laser,” Opt. Lett., 32, 2559-2561 (2007)
[15] Itoh, K. “Ultrafast Laser Processing of Glass,” JLMN J. of Laser Micro/Nanoengineering, 3, 187 – 191 (2014)
[16] Kumkar, M., Bauer, L., Russ, S., Wendel, M., Kleiner, J., Grossmann, D., Bergner, K., Nolte, S., “Comparison of different processes for separation of glass and crystals using ultrashort pulsed lasers,” Proc. of SPIE, 8972, (2014)
[17] Hartmann, C. A., Fehr, T., Braydic, M., Gillner, A., ”Investigations on Laser Micro Ablation of Steel Using Short and Ultrashort IR Multipulses,” JLMN J. of Laser Micro/Nanoengineering, 2, 44 – 48 (2007)
[18] Knappe, R., Haloui, H., Seifert, A., Weis, A., Nebel, A., ”Scaling ablation rates for picosecond lasers using burst micromachining,” Proc. of SPIE, 7585, (2010)
[19] Hu, W., Shin, Y.C., King, G., “Modeling of multi-burst mode pico-second laser ablation for improved material removal rate,” Appl. Phys. A, 98, 407 – 415 (2009)
[20] Chichkov, B.N., Momma, C., Nolte, S., van Alvensleben, F., Tünnermann, A., “Femtosecond, picosecond and nanosecond laser ablation of solids,” Applied Physics A, 63, 109-115 (2001)
[21] Mannion, P., Magee, J., Coyne, E., O’Conner, G.M., “Ablation thresholds in ultrafast laser micro-machining of common metals in air,” Proceedings of SPIE, 4876, 470 – 478 (2003)
[22] Bauer, F., Michalowski, A., Kiedrowski, Th., Nolte, S., “Heat accumulation in ultra-short pulsed scanning laser ablation of metals,” Opt. Expr., 23, 1035 – 1043 (2015)
[23] Koenig, J., Nolte, S., Tuennermann, A., “Plasma evolution during metal ablation with ultrashort laser pulses,“ Opt. Expr., 26, 10597 – 10607 (2005)
[24] Brueckner, M., Schaefer, J.H., Uhlenbusch, J., “Ellipsometric measurement of he optical constants of solid and molten aluminum and copper at l=10.6μm,” J. Appl. Phys., 66, 1326 (1989)